Sensitivity Analysis of a Phenomenological Thrombosis Model and Growth Rate Characterisation

Gian Marco Melito[1], Alireza Jafarinia[2], Thomas Hochrainer[2], Katrin Ellermann[1]

[1]University of Technology Graz, Institute of Mechanics
Kopernikusgasse 24/IV, Graz, Austria 8010
gmelito@tugraz.at; ellermann@tugraz.at

[2]University of Technology Graz, Institute of Strength of Materials
Kopernikusgasse 24/I, Graz, Austria 8010
alireza.jafarinia@tugraz.at; hochrainer@tugraz.at

Abstract - *Aortic dissection is a severe cardiovascular disease caused by the occurrence of a tear in the aortic wall. As a result, the blood penetrates the wall and makes a new blood channel called the false lumen. The haemodynamic conditions in the false lumen may contribute to the formation of thrombi, which influence the patient's diagnosis and outcomes. In this study, the focus is on a haemodynamic-based model of thrombus formation. Since the model construction entails uncertainties in the model parameters, a variance-based sensitivity analysis is performed. Thrombus formation at a backward-facing step is considered as a benchmark for the numerical simulations and sensitivity analysis. This geometry is capable of representing the main contributions of the model in thrombus formation. The study aims at improving the understanding of the model's structure and at preparing model simplifications to enable efficient patient-specific simulations in the future. A polynomial chaos expansion is employed as a surrogate model, from which the quantitative sensitivity indices are derived. In this study, nine model parameters are selected, whose proper values are not well known. The model responses taken into account are the maximum volume fraction of thrombus, its time development, and the thrombus growth rate. The results show that the model lends itself to model reduction since some of the model parameters show little to no influence on the model's outputs. A threshold value related to the concentration of bounded platelets and the bounded platelets reaction rate are identified as the key input parameters dominating the thrombus model predictions in the current geometry. Furthermore, the introduced thrombus characteristic growth time is driven by both the aforementioned variables.*

Keywords: Aortic Dissection, Thrombus Formation, Global Sensitivity Analysis, Backwards-Facing Step.

Nomenclature

Symbol	Description
Thrombus formation model	
T_R	Residence time, s
T_{Rt}	Residence time threshold, s
D_{T_R}	Diffusion coefficient, $\mathrm{m^2 s^{-1}}$
c_i	Concentration of resting or activated platelets, $\mathrm{m^{-3}}$
RP	Resting platelets, $\mathrm{m^{-3}}$
AP	Activated platelets, $\mathrm{m^{-3}}$
D_P	Diffusion coefficient of platelets, $\mathrm{m^2 s^{-1}}$
s_i	Reaction term for platelets conversion, $\mathrm{m^{-3} s^{-1}}$
c	Coagulant concentration, $\mathrm{mol\ m^{-3}}$
c_t	Coagulant concentration threshold, $\mathrm{mol\ m^{-3}}$
$D_{c_{eff}}$	Effective coagulant diffusivity, $\mathrm{m^2 s^{-1}}$
k_c	Coagulant kinetic constant, $\mathrm{mol\ m^{-3} s^{-1}}$
k_{th}	Constant coefficient in N-S equation sink term, $\mathrm{kg m^{-3} s^{-1}}$
c_{BP}	Concentration of bounded platelets, $\mathrm{mol\ m^{-3}}$
c_{BPt}	Concentration of bounded platelets threshold, $\mathrm{mol\ m^{-3}}$

c_{BPbt}	Bounded platelets concentration threshold at the wall, mol m^{-3}	
$k_{\text{c,wall}}$	Coagulant kinetic constant at the wall, $\text{mol m}^{-2}\text{s}^{-1}$	
D_{c}	Coagulant diffusivity, m^2s^{-1}	
k_{BP}	Bounded platelets reaction rate, $\text{mol m}^{-3}\text{s}^{-1}$	
c_{AP}	Concentration of activated platelets, m^{-3}	
t_{c}	Characteristic growth time, s	
$\dot{\Phi}_{c}$	Characteristic growth rate, $\text{m}^3 s^{-1}$	

Fluid mechanics

$\boldsymbol{u}$	Velocity vector, ms^{-1}
$\dot{\gamma}$	Shear rate, s^{-1}
$\dot{\gamma}_{\text{t}}$	Shear rate threshold, s^{-1}
ρ	Blood density, kgm^{-3}
μ	Blood viscosity, m^2s^{-1}
p	Fluid pressure, Pa
$\boldsymbol{\tau}$	Extra stress tensor, Pa
R_{L}	Reattachment length, m

Model geometry

S	Step depth, m
H	Inlet height, m
L	Total length, m
V	Domain volume, m^3

Sensitivity analysis

Y	Quantity of interest
f	Computational model
$\boldsymbol{x}$	Input random vector
x_{i}	Input random variable
n	Model dimension
$\mathbb{E}[\cdot]$	Mean operator
$\mathbb{V}[\cdot]$	Variance operator
S_{i}	First-order sensitivity index
S_{i}^{T}	Total-order sensitivity index
f_{PCE}	Polynomial chaos expansion function
y_{α}	Expansion coefficient
$\boldsymbol{\Psi}_{\alpha}$	Multivariate polynomial
α	Multi-indices of polynomial expansion
A	Set of multi-indices
N_{s}	Number of samples

1. Introduction

Aortic dissection (AD) is a disease that develops a second volume, called false lumen (FL), in the aorta. AD is classified as type A when it initiates in the ascending thoracic aorta, type B when the initial tear in the aortic wall is in the descending thoracic aorta (Stanford Classification System). Type B aortic dissection (TBAD) is a severe disease associated with high mortality, which may also lead to complications such as aortic aneurysm, rupture or malperfusion syndromes [1]. In the current study, the focus is on TBAD and the role of thrombosis in the false lumen.

The haemodynamic conditions in the FL, including flow disturbance, recirculations, and significant variability in the wall shear stress (WSS) presumably promote the formation and growth of thrombi [2]. In [3], it is shown that partial thrombosis is associated with a higher mortality rate, whereas complete thrombosis of the FL improves patients' prognosis [4], [5]. Up to now, it is not entirely clear what circumstances favour thrombosis following aortic dissection. Thrombus formation models may play a vital role in the analysis of haemodynamics in cardiovascular environments.

In [2] and [6], a haemodynamic-based model capable of predicting false lumen thrombosis in TBAD is developed. However, because the model is mostly phenomenological, the parameters of the model may not be determined from chemical or biological characteristics of the blood. Instead, the parameters will usually be obtained from inverse modelling, i.e. fitting to measured data. However, suitable time-resolved data of thrombus-formation is very sparse, which is why it is of vital importance to narrow down the number of model parameters. A global sensitivity analysis is suggested to understand the influence of the parameters [7].

The model performs well in predicting the location of thrombus formation; however, it is unable to reproduce the growth rate as observed in in-vivo and in-vitro studies. More insight into the model parameters and their role in thrombus growth is needed to bridge the gap between numerical simulations and real-life studies. This paper identifies the most critical parameters for the thrombus growth model, and further analysis of the thrombus characteristic growth time indicates the parameters that could accelerate or inhibit the process of thrombus formation.

The paper is structured as follows: the thrombus formation model is exposed in Section 2, the theory of sensitivity analysis is explained in Section 3, while its application to the computational model is in Section 3.2. Results of the analysis and the conclusions are exposed in Sections 4 and 5, respectively.

2. Thrombus Formation and Growth

In this study, the thrombus formation model developed in [2] is used. It is a haemodynamic-based model in which the thrombus forms and grows mainly in areas where low shear stress and high residence time are measured. The model consists of the following equations, which are coupled with Navier-Stokes equations. The residence time T_R is a field quantity, which obeys the following evolution law,

$$\frac{\partial T_R}{\partial t} + \boldsymbol{u} \cdot \boldsymbol{\nabla} T_R = D_{T_R} \boldsymbol{\nabla}^2 T_R + 1, \tag{1}$$

where $\boldsymbol{u}$ denotes the velocity vector, and D_{T_R} is a diffusion coefficient. High T_R marks areas where platelets spend more time [2]. The transport equation for the concentration c_i of resting or activated platelets (RP or AP, resp.) is

$$\frac{\partial c_i}{\partial t} + \boldsymbol{u} \cdot \boldsymbol{\nabla} c_i = D_P \boldsymbol{\nabla}^2 c_i + s_i, \quad i = RP, AP. \tag{2}$$

Here, D_P denotes the diffusion coefficient of platelets, which is the same for resting and activated platelets. Furthermore, s_i denote reaction terms for the conversion of resting to activated platelets [2].

The so-called coagulant concentration c accounts for the lumped effect of all underlying biochemical reactions in the coagulation cascade [2]. In low shear rate areas, there is a production of coagulant at the wall based on the conditions specified on the boundary, compare Eq. (5). This modified boundary condition for the flux of coagulant is taken from [6] for the backwards-facing step. The diffusion-reaction equation for the coagulant is

$$\frac{\partial c}{\partial t} = D_{c_{eff}} \boldsymbol{\nabla}^2 c + k_c \phi_{th} \phi_{\dot{\gamma}}, \tag{3}$$

where k_c is the coagulant kinetic constant, $\dot{\gamma}$ is the shear rate. Furthermore,

$$\phi_{\dot{\gamma}} = \dot{\gamma}_t^2 / (\dot{\gamma}^2 + \dot{\gamma}_t^2), \tag{4}$$

where the subscript t denotes the threshold values, and

$$D_{c_{eff}} \frac{\partial c}{\partial n}\bigg|_{wall} = \begin{cases} 0, & \text{if } \dot{\gamma} > 1 \, s^{-1}, c_{BP} > 200 \text{ nM} \\ k_{c,wall}, & \text{else.} \end{cases}, \tag{5}$$

The effective coagulant diffusivity $D_{c_{eff}}$ is proportional to the coagulant diffusivity D_c,

$$D_{c_{eff}} = \phi_{\dot{\gamma}} D_c. \tag{6}$$

Finally, the rate of production of bounded platelets concentration c_{BP} is given by

$$\frac{\partial c_{BP}}{\partial t} = k_{BP} \phi_{BP} \phi_{\dot{\gamma}} c_{AP}, \tag{7}$$

where

$$\phi_{BP} = \left(\frac{c^2}{c^2 + c_t^2}\right)\left(\frac{T_R^2}{T_R^2 + T_{Rt}^2}\right). \tag{8}$$

Here, k_{BP} denotes the bounded platelets reaction rate and c_{AP} is the activated platelets concentration. The Navier-Stokes equation is modified to incorporate the thrombus growth [2]

$$\rho\left[\frac{\partial u}{\partial t} + (\boldsymbol{u} \cdot \boldsymbol{\nabla})\boldsymbol{u}\right] = -\boldsymbol{\nabla} p + \boldsymbol{\nabla} \cdot \boldsymbol{\tau} - k_{th} \phi_{th} \boldsymbol{u}, \tag{9}$$

where ρ denotes the blood density, p the pressure, $\boldsymbol{\tau}$ is the extra stress tensor, and

$$\phi_{th}(c_{BP}, c_{BPt}) = \frac{c_{BP}^2}{c_{BP}^2 + c_{BPt}^2}. \tag{10}$$

The quantity ϕ_{th} indicates local thrombosis as a function of the bounded-platelets concentration c_{BP} and its threshold c_{BPt}. Furthermore, k_{th} is a coefficient with a sufficiently high value to stop the flow where the thrombus is formed [2]. In summary, the model controls the formation of thrombus based on shear stress, residence time, the concentration of coagulant and platelets.

3. Numerical Simulations

OpenFOAM software is used for solving the blood flow and thrombus formation equations. The *blockMesh* utility in OpenFOAM is used for generating a structured hexahedral mesh. Blood is modelled as a Newtonian fluid. The geometry is characterised by a step depth (S) of 2.5 mm, inlet height (H) of 7.5 mm and a total length (L) of 120 mm.

3. 1. Initial and Boundary Conditions

For the inlet boundary condition of the velocity, a uniform velocity profile resulting in Reynolds number of 490 was imposed, with the no-slip condition for the walls. The pressure gradient is equal to zero on all the boundaries except the outlet, which is considered having a fixed value of zero.

As discussed in sections 2, there are five equations to be solved for the thrombus formation model. For solving residence time T_R equation (Eq. 1), which is initially zero, the inlet value of T_R is fixed to zero, and the normal gradient on all the other boundaries is set to zero.

Initial values of resting platelets RP and activated platelets AP in the blood are taken from [2]. The inlet values of RP and AP (Eq. 2) are fixed to their initial values. Zero normal gradients of AP and RP is imposed on all the other boundaries. For the coagulant equation (Eq. 3), the Neumann boundary condition discussed in section 2 is implemented for the walls, while a zero fixed value at the inlet and a zero normal gradient at the outlet are applied. Bounded platelets equation (Eq. 7) is solved with zero initial concentration of bounded platelets.

3. 2. Backward-facing step benchmark

The thrombus formation simulation starts at 12 seconds from the steady-state flow solution. A Reynolds number of 490 is chosen to be consistent with in-vitro results in [8] and numerical simulations in [9]. To test the performance of numerical simulations, the reattachment length R_L at the back of the step for four Reynolds numbers is compared to the numerical results of [10]. For this comparison, the expansion ratio of $1 + S/H = 2$ is adopted [10]. The Reynolds number Re is computed as

$$Re = \frac{\rho U D_h}{\mu} \tag{11}$$

where U is inlet velocity, D_h is the hydraulic diameter and equal to $2H$ [10], $\rho = 1060\,\text{kg/m}^3$ is the blood density, and blood viscosity $\mu = 4.7 \times 10^{-3}\,\text{m}^2/\text{s}$ [9].

Figure 1 shows that the present results are in good agreement with the benchmark solutions [10]. Mesh and time-step sensitivity analysis resulted in 20,000 elements and a time-step of 0.005s.
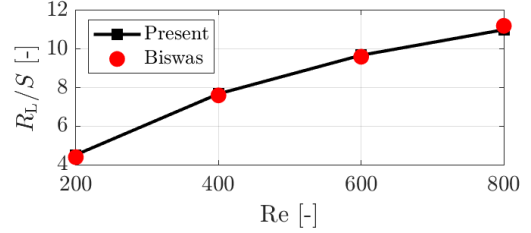

Figure 1. Normalised reattachment length with respect to step height versus Reynolds numbers

3. 3. Thrombus formation model

In Figure 2, the recirculation area behind the step is highlighted by the streamlines superposed on a density plot of the magnitude of the fluid velocity. The model predicts thrombus formation in the recirculation area behind the step which qualitatively matches with in-vitro results in [8] and numerical simulations in [9], see Figure 3.
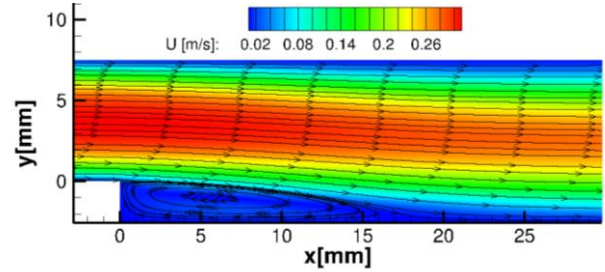

Figure 2. Streamlines and magnitude of velocity indicating recirculation at the back of the step.
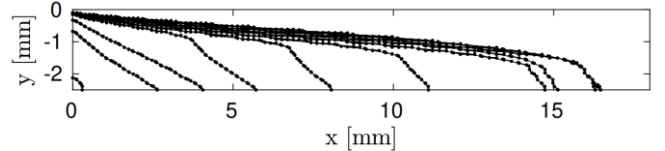

Figure 3. Evolution of thrombus in time at the back of the step. The thrombus has reached 16 mm length in 50 s.

4. Sensitivity analysis

Consider a quantity of interest Y of computational model f function of an input random vector $\boldsymbol{x}$ of dimension n, i.e. $Y = f(\boldsymbol{x}) = f(x_1, x_2, \dots, x_n)$. One of the most widely used technique in global sensitivity analysis is the variance-based method, which quantifies the connection between the variance of the model output Y, given the variability of its inputs x_i. The sensitivity analysis may be employed for model reduction, in that the non-influential variables of a computational model may be considered constants. Furthermore, sensitivity analysis enables input factor prioritisation, by ranking the parameters, to which the outcome is most sensitive.

A random variable x_i is considered to be influential (non-influential) to the model f with output Y if the conditional variance $\mathbb{V}\big[\mathbb{E}[Y|x_i]\big]$ is larger (smaller) than the variance of the quantity of interest $\mathbb{V}[Y]$, where $\mathbb{V}[\cdot]$ and $\mathbb{E}[\cdot]$ represent the variance and the mean operators. The first-order sensitivity index (or first-Sobol index) is defined as [11]

$$S_i = \frac{\mathbb{V}\big[\mathbb{E}[Y|x_i]\big]}{\mathbb{V}[Y]}. \tag{12}$$

The first-Sobol index represents the contribution of the random variable x_i, for $1 \leq i \leq n$, to the change of the model output Y.

The total-order sensitivity index (or total-Sobol index) is defined as

$$S_i^{\mathrm{T}} = 1 - \frac{\mathbb{V}\big[\mathbb{E}[Y|x_{\sim i}]\big]}{\mathbb{V}[Y]} = \frac{\mathbb{E}\big[\mathbb{V}[Y|x_{\sim i}]\big]}{\mathbb{V}[Y]}. \tag{13}$$

The total-Sobol index evaluates the total effect of an input parameter, by accounting for the conditional variance of the output, conditioning to all factors except the given one, $x_{\sim i}$.

The first-Sobol index identifies the level of influence of a single parameter on the output in the analysis, but it does not give information regarding the interaction of the parameter with other variables of the input space. It may be used for factor prioritisation, where a ranking of the parameters is produced. The rank indicates the level of influence on the model variation, and therefore it highlights the input uncertainty that needs to be removed. The total-order sensitivity index specifies the influence of the input parameter on the model output and the level of interaction with other input parameters. The total-order index is used for factor fixing. Here, the lower values are considered to decide which variable has no- or low-effect on the output. Such variables can be successively considered as model's constant.

4. 1. Polynomial Chaos Expansion

The Sobol indices are assessed from a polynomial chaos expansion (PCE) of the computational model [12].

PCE consists of the sum of orthogonal, multivariate polynomials Ψ_α of increasing order up to some maximal polynomial order p [13]. The polynomials are multiplied by expansion coefficients y_α, which can be estimated with different methods. The expansion is written as

$$Y(\boldsymbol{x}) \approx f_{\mathrm{PCE}}(\boldsymbol{x}) = \sum_{\alpha \in A} y_\alpha \boldsymbol{\Psi}_\alpha(\boldsymbol{x}), \tag{14}$$

where A is a set of multi-indices α which refer to the degree of each polynomial with respect to each input parameter. The multivariate polynomials $\boldsymbol{\Psi}_\alpha$ are defined as the product of univariate polynomials of order α_i, i.e. ψ_{α_i}. The univariate polynomials are generated following the Askey scheme [14] for the composition of polynomials.

Finally, from the PCE, it is possible to estimate the two sensitivity indices as the ratio between the PCE coefficients [14]. Since the case study is dynamic, the variance of the output evolves in time. A pointwise-in-time evaluation of sensitivity indices turns out to be inaccurate in describing such evolution. Therefore, an analysis that is aware of the history of the output variability is needed. The implementation of time-dependent indices, known as generalised Sobol indices [15] reads

$$S_i(t) = \frac{\int_0^t \mathbb{V}_i[Y(x_i, \tau)]d\tau}{\int_0^t \mathbb{V}[Y(\boldsymbol{x}, \tau)]d\tau} \approx \frac{\sum_{\alpha \in A_i} y_\alpha^2(t)}{\sum_{\alpha \in A_i; \alpha \neq 1} y_\alpha^2(t)}$$
$$= \frac{\int_0^t \sum_{\alpha \in A_i} y_\alpha^2(\tau)\, d\tau}{\int_0^t \sum_{\alpha \in A_i; \alpha \neq 1} y_\alpha^2(\tau)\, d\tau}, \tag{15}$$

$$S_i^{\mathrm{T}}(t) \approx \frac{\sum_{\alpha \in A_i^{\mathrm{T}}} y_\alpha^2(t)}{\sum_{\alpha \in A_i; \alpha \neq 1} y_\alpha^2(t)}$$
$$= \frac{\int_0^t \sum_{\alpha \in A_i^{\mathrm{T}}} y_\alpha^2(\tau)\, d\tau}{\int_0^t \sum_{\alpha \in A_i; \alpha \neq 1} y_\alpha^2(\tau)\, d\tau}. \tag{16}$$

4. 2. Application to the thrombus formation model

The input parameters that are considered to represent uncertainty are listed in Table 1. To adequately cover and understand the sensitivity of thrombus formation on the selected parameters, the volume fraction of thrombus, the thrombus growth rate, and a characteristic growth time t_c are considered as the quantities of interest. The volume fraction of thrombus expressed as a percentage is defined as

$$\bar{\phi}_{\mathrm{th}}(t) = \frac{1}{V} \int_V \phi_{\mathrm{th}}(x, y, z, t)dV * 100, \tag{17}$$

where V is the domain volume and the thrombus growth rate ($\%/s$) as

$$\dot{\bar{\phi}}_{th}(t) = \frac{d}{dt}\big(\bar{\phi}_{th}(t)\big). \tag{18}$$

It seems promising to introduce an indicator that describes the development of the thrombus in time. This indicator could improve model fitting to experimental data, the introduction of a time scale in thrombus growth, or both. A characteristic growth time t_c is therefore introduced, which is defined by the maximum peak of the thrombus growth rate, thus the time after which the thrombus growth rate decreases significantly. At t_c the thrombus formation is considered almost complete, and the thrombus is said to be developed, i.e. its volume will no longer change significantly in time. An example of t_c identification is illustrated in Figure 4, where the growth rate of one typical simulation is plotted over the simulation time. The characteristic growth time t_c is unique for each simulation. However, not all simulations reached a growth rate peak in the simulation time, preventing the assignment of the characteristic growth time. Such simulations were excluded from the sensitivity analysis.
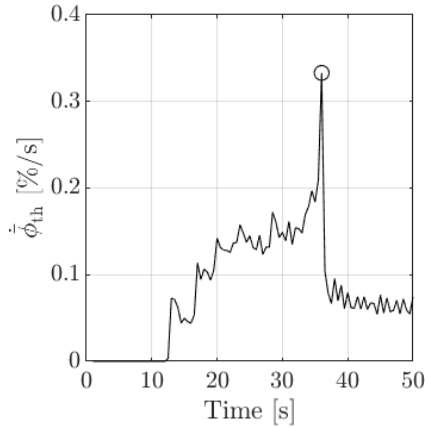

Figure 4. Example of thrombus growth rate in time. A black circle indicates the characteristic growth time t_c.

The developed thrombus and its characteristic growth time are directly connected. Acceleration or deceleration of the thrombus formation results in a variation of t_c in the model. For an in-depth understanding of the growth characteristics, this relationship should be analysed in detail.

Each model input factor is treated as a uniformly distributed random variable on a given interval, since their actual values, and distributions are not known,

Table 1. The sample is produced with latin hypercube sampling techniques with size N_s equal to 450. The number of simulations is bounded by the high computational cost of the model and fulfils the requirements for the construction of the PCE. The latter is solved with the regression LARS method through the Matlab toolbox UQlab [16], where the degree of the polynomial is set to 3.

5. Results

The sensitivity indices S_i and S_i^T for the maximum volume fraction of thrombus are listed in Table 2. By looking at the first column, one observes that the first-order sensitivity indices do not sum up to one, which occurs in the presence of non-additive model behaviour. Circa 90% of the output variance can be attributed to c_{BPt}, k_{BP}, and c_{AP}. The bounded platelets threshold c_{BPt} accounts alone, i.e. without considering interactions, for about 64% of the variation of the volume fraction of thrombus. By subtracting the first-order from the total-order indices of Table 2, the interaction effect is estimated.

Table 1. Input parameters of the thrombus model and their probabilistic distribution used for the sensitivity analysis. All input parameters follow a uniform probability distribution on the indicated interval.

Parameters	Name	PDF parameters
Activated platelets concentration	c_{AP}	[1.00e-10, 1.00e-06]
Coagulant diffusivity	D_c	[2.00e+04, 2.00e+06]
Coagulant kinetic constant	k_c	[8.00e-11, 8.00e-09]
Bounded platelets reaction rate	k_{BP}	[1.00e+03, 1.00e+05]
Coagulant concentration threshold	c_t	[2.00e+03, 2.00e+05]
Bounded platelets concentration threshold	c_{BPt}	[1.00e-01, 3.00e+00]
Coagulant kinetic constant at the wall	$k_{c,wall}$	[1.00e+02, 1.00e+05]
Residence time threshold	T_{Rt}	[0.750e+13, 2.25e+13]
Bounded platelets concentration threshold at the wall	c_{BPbt}	[1.00e+02, 2.50e+05]

Since the thrombus develops in time, it is essential to understand how the variation of its development evolves in time. The results show several trends (Figures 5 and 6). Increasing variability in time is visible, especially towards the end of the simulation time. In Figure 5, at 50 s of simulation time, the distribution of the recorded maximum volume fraction of thrombus varies from the absence of thrombus to a thrombus coverage of circa 30% of the volume domain. Such variability is critical for a model in which the computation of the thrombus volume is an important goal.

The results of the generalised total-Sobol indices for the volume fraction of thrombus and the thrombus growth rate are shown in Figure 7. The sensitivity analysis results do not differ for the two quantities of interest (Eq.17 and 18); therefore, only one plot is shown. Furthermore, the first-Sobol index does not display a trend that differs from the total-Sobol index, suggesting a low degree of interactions between the input random variables [17]. In Figure 7, the sensitivity analysis in time of volume fraction of thrombus and thrombus growth rate shows the significant influence of the bounded platelets concentration threshold c_{BPt}. Besides this, only the bounded platelets reaction rate k_{BP} shows a comparably strong effect on the volume fraction of thrombus.

The other input random variables mostly have a small or negligible effect on the output and might be considered as model constants. The only exception is the significant role of the residence time threshold T_{Rt} in the early stage of thrombus initiation.

Table 2: Sobol indices of the input random variables on the maximum volume fraction of thrombosis.

x_i	S_i	S_i^T	$S_i^T - S_i$
c_{BPt}	0.638	0.730	0.093
k_{BP}	0.198	0.277	0.078
c_{AP}	0.043	0.060	0.017
D_c	0.012	0.017	0.004
T_R	0.007	0.014	0.007
$k_{c,wall}$	0.001	0.008	0.007
c_{BPbt}	0.000	0.005	0.004
c_t	0.000	0.005	0.005
K_c	0.000	0.001	0.001
Total	0.900	1.117	0.218

However, this parameter is mostly responsible for sparking off the formation of the thrombus, while its effect on the final thrombus size is also negligible. The

influence of the coagulant diffusivity D_c shows a small peak right after the first formation of the thrombus, but remains low throughout the simulation time.

As may be read from Eq. 7 and Eq. 8, bounded platelets are generated from activated platelets in areas with low shear rate, high residence time and high concentration of coagulant. The bounded platelets can stop the flow if their concentration is sufficiently higher than the threshold value, c_{BPt}. Any variation of the bounded platelets concentration threshold will significantly change the process of thrombus formation, i.e. it essentially controls where and how fast the thrombus can form. Moreover, the reaction rate k_{BP} determines how fast the concentration of bounded platelets may reach the threshold value c_{BPt}.
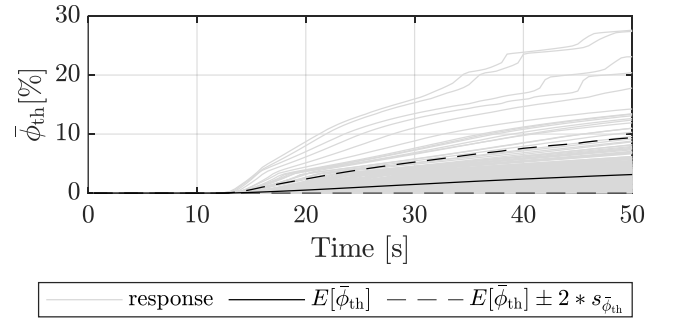

Figure 5. Volume fraction of thrombus. The continuous line shows the mean value; the dashed line represents the 2 standard deviations of the data.
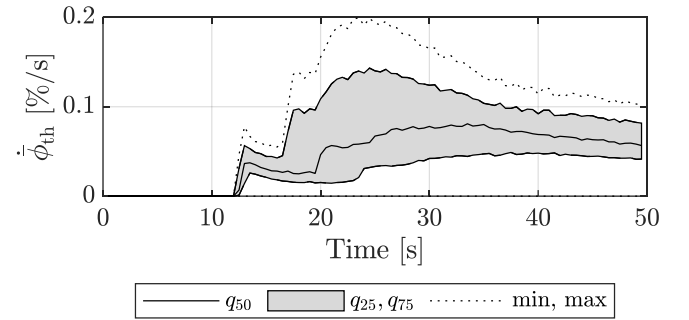

Figure 6. Thrombus growth rate in time. The central continuous black line identifies the median value; the grey area represents the interquartile range; the dotted lines are the maximum and minimum data points.

The interconnected roles of the two parameters k_{BP} and c_{BPt} on thrombus formation advocate the idea that there might be a correlation between these parameters and a characteristic time of the thrombus formation process. To verify if the characteristic growth time t_c is the right candidate for characterising the

thrombus growth rate, a sensitivity analysis is also performed for this quantity of interest.

The sensitivity analysis results for the characteristic growth time t_c of the thrombus are shown in Figure 8. Here, the sensitivity indices are shown in a bar plot, where the first- and total-Sobol indices are shown side-by-side to highlight the presence of potential interactions, given by their difference in value. The main parameters affecting the shift in t_c are again the bounded platelets concentration threshold c_{BPt} and the bounded platelets reaction rate k_{BP}.
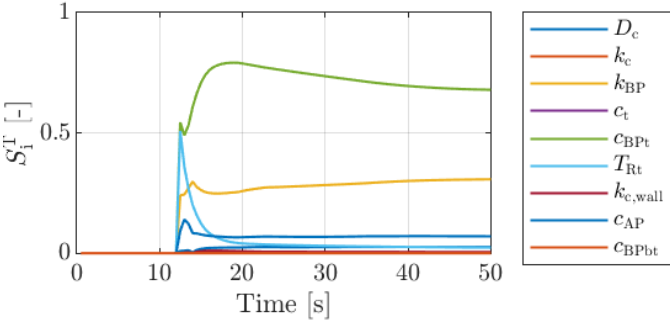

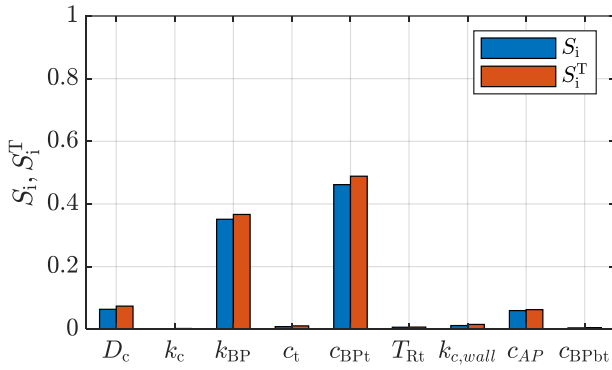Figure 7. Generalised total-Sobol index for the volume fraction of thrombus $\bar{\phi}_{th}(t)$.

Figure 8. Sensitivity analysis results for the characteristic growth time of thrombus t_c.

From the results of the sensitivity analysis for t_c (Figure 8), the characteristic growth time is a function of c_{BPt} and k_{BP}. Because a high threshold c_{BPt} delays thrombus growth, while a high reaction rate k_{BP} has an accelerating effect, the ratio between them is introduced as a characteristic growth rate $\dot{\Phi}_c$ of the model,

$$\dot{\Phi}_c = \frac{k_{BP}}{c_{BPt}}, \tag{18}$$

with the dimension of a cubic meter per second (m^3/s). Its relationship to the characteristic growth time t_c is shown in Figure 9. Here, the data are produced with the computation of the metamodel for the characteristic growth time considering all input parameters, except for c_{BPt} and k_{BP}, as constants. The data was fit with non-linear regression. A low value of the characteristic growth rate $\dot{\Phi}_c$ leads to high values of t_c, that can be interpreted as a delayed thrombus growth. Such behaviour is a consequence of a low value of bounded platelets reaction rate k_{BP}, and a high bounded platelets concentration threshold c_{BPt}. In the case of high c_{BPt}, the required number of bounded platelets to form a thrombus has to be higher, and therefore its growth is reduced.

The data have been fitted by

$$t_c \frac{U}{H} = a \left(\frac{\dot{\Phi}_c}{Q} \right)^b, \tag{19}$$

where U/H is the model convection time given by the ratio of inlet velocity magnitude U and inlet height H, $Q = U * A$ is the volumetric flow rate, where the area A is the product of inlet height H and geometry depth 1 m. The constants a and b are computed by non-linear regression analysis. Their values, together with their 95% confidence intervals, are: $a = 0.33 \pm 2.21 \cdot 10^{-2}$, and $b = -3.36 \cdot 10^{-1} \pm 2.80 \cdot 10^{-3}$. The coefficient of determination $R^2 = 0.93$.
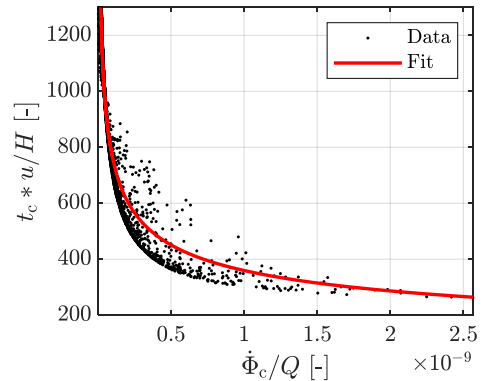

Figure 9. Variation of characteristic growth time of thrombus t_c normalised by convection time u/H as a function of the characteristic growth rate $\dot{\Phi}_c$ normalised by volumetric flow rate Q.

Such a formulation of the characteristic growth time of the thrombus appears as a promising tool for the modelling phase. By varying the characteristic growth

rate of the problem, it is possible to accelerate or inhibit the thrombus formation.

6. Conclusions

The thrombus formation model presents a high amount of variation due to the intrinsic uncertainty of the input parameters, which are usually collected from different literature sources. The input variation is modelled with uniform probability distributions for nine model input random variables, and a sensitivity analysis is performed through the construction of a polynomial chaos expansion metamodel. To better grasp the model variation for the scope of the study, the quantities of interest are considered to be the volume fraction of thrombus, the thrombus growth rate, and the time instant at which the growth rate peak is recorded, namely the characteristic growth time.

Input parameters such as the bounded platelets reaction rate k_{BP} and the bounded platelets concentration threshold of activated platelets c_{BPt}, show high sensitivity indices, and therefore their proper determination requires further investigation. In general, the input parameters that include the platelet's mechanics control most of the process, except for the bounded platelets threshold at the boundary c_{BPbt}. All the other input random variables, including the parameters relating to the coagulant, have little to no influence on the considered outputs, and therefore they could be switched to fixed values without altering the model response.

The results of the sensitivity analysis for the model outputs show that the bounded platelets threshold c_{BPt} exerts the most substantial influence. The reaction rate of bounded platelets k_{BP} plays the second-largest role in the thrombus growth rate and the volume fraction of thrombus.

Finally, the introduced characteristic growth rate k_{BP}/c_{BPt} appears to be a promising indicator for the speed of thrombus formation. This characteristic rate is supposed to be beneficial for fitting model results to experimental results, in-turn improving the haemodynamic-based model in predicting thrombus formation on a proper time scale.

Acknowledgement

References

[1] C.A. Nienaber, R.E. Clough, N. Sakalihasan, T. Suzuki, R. Gibbs, F. Mussa, M.P. Jenkins, M.M. Thompson, A. Evangelista, J.S.M. Yeh, N. Cheshire, U. Rosendahl & J. Pepper "Aortic dissection". In: *Nature Reviews* Disease Primers 2.1 (2016), pp. 1-18.

[2] C. Menichini and X.Y. Xu. "Mathematical modeling of thrombus formation in idealised models of aortic dissection: initial findings and potential applications". In: *Journal of mathematical biology* 73.5 (2016), pp. 1205-1226.

[3] T.T. Tsai, A. Evangelista, C.A. Nienaber, T. Myrmel, G. Meinhardt, J.V. Cooper, D.E. Smith, T. Suzuki, R. Fattori, A. Llovet, J. Froehlich, S. Hutchison, A. Distante, T. Sundt, J. Beckman, J.L. Januzzi, E.M. Isselbacher, K.A. Eagle. "Partial thrombosis of the false lumen in patients with acute type B aortic dissection". In: *New England Journal of Medicine* 357.4 (2007), pp. 349-359.

[4] Y. Bernard, H. Zimmermann, S. Chocron, J-F. Litzler, B. Kastler, J-P. Etievent, N. Meneveau, F. Schiele, J-P. Bassand. "False lumen patency as a predictor of late outcome in aortic dissection". In: *The American journal of cardiology* 87.12 (2001), pp. 1378-1382.

[5] S. Trimarchi, J.L. Tolenaar, F.H.W. Jonker, B. Murray, T.T. Tsai, K.A.Eagle, V. Rampoldi, H.J.M. Verhagen, J.A.van Herwaarden, F.L. Moll, B.E. Muhs, J.A. Elefteriades *Importance of false lumen thrombosis in type B aortic dissection prognosis*. 2013.

[6] C. Menichini, Z.Cheng, R.G.J. Gibbs and X.Y. Xu "Predicting false lumen thrombosis in patients-specific models of aortic dissection". In: *Journal of The Royal Society Interface* 13.124 (2016), p. 20160759.

[7] B. Sudret. "Global sensitivity analysis using polynomial chaos expansions". In: *Reliability engineering & system safety* 93.7 (2008), pp. 964-979.

[8] J.O. Taylor, K.P. Witmer, T. Neuberger, B.A. Craven, R.S. Meyer, S. Deutsch, K.B. Manning "In vitro quantification of time dependent thrombus size using magnetic resonance imaging and computational simulations of thrombus surface shear stresses". In: *Journal of biomechanical engineering* 136.7 (2014).

[9] J.O. Taylor, R.S. Meyer, S. Deutsch, K.B. Manning "Development of a computational model for

macroscopic predictions of device-induced thrombosis". In: *Biomechanics and modeling in mechanobiology* 15.6 (2016), pp. 1713-1731.

[10] G. Biswas, M. Breuer, F. Durst. "Backward-facing step flows for various expansion ratios at low and moderate Reynolds numbers." *J. Fluids Eng.* 126, no. 3 (2004): 362-374.

[11] I. M. Sobol. "Global sensitivity indices for nonlinear mathematical models and their Monte Carlo estimates". In: *Mathematics and computers in simulation* 55.1-3 (2001), pp. 271-280.

[12] R. G. Ghanem, P. D. Spanos. *Stochastic Finite elements: a spectral approach*. Courier Corporation, 2003.

[13] D. Xiu and G. E. Karniadakis. "The Wiener-Askey polynomial chaos for stochastic differential equations". In: *SIAM journal on scientific computing* 24.2 (2002), pp. 619-644.

[14] T. Crestaux, O. Le Maître, and J. Martinez. "Polynomial chaos expansion for sensitivity analysis". In: *Reliability Engineering & System Safety* 94.7 (2009), pp. 1161-1172.

[15] A. Alexanderian, P. A. Gremaud, and R. C. Smith. "Variance-based sensitivity analysis for time-dependent processes". In: *Reliability Engineering & System Safety*, 196 (2020), pp. 106722.

[16] S. Marelli and B. Sudret. "UQLab: A framework for uncertainty quantification in Matlab". In: *Vulnerability, uncertainty, and risk: quantification, mitigation, and management*. 2014, pp. 2554-2563.

[17] Melito, G. M., Jafarinia, A., Hochrainer, T., & Ellermann, K. (2020, July). "Sensitivity analysis of a hemodynamic-based model for thrombus formation and growth". In: *Proceedings of the 6th World Congress on Electrical Engineering and Computer Systems and Sciences (EECSS'20): ICBES'20* (2020), pp. ICBES-127.